Electronic Supplementary Material (ESI) for RSC Advances.
This journal is © The Royal Society of Chemistry 2016

Simultaneous Enhancement in Stability and Efficiency of Low-Temperature Processed Perovskite Solar Cells

SUPPORTING INFORMATION

Table S1: Peak width and estimated dimension of individual crystallite of ZnO and AZO film calculated by the spectral fitting from XRD measurement data

ETL Layer	(002) Crystal Orientation		(101) Crystal Orientation	
	Peak Width (nm)	Crystallite Size (nm)	Peak Width (nm)	Crystallite Size (nm)
Pristine ZnO	0.32827	5.39	0.72964	2.50
Al doped ZnO (AZO)	0.40161	4.41	0.82925	2.19

Table S2: Average photovoltaic performance of $MA_{0.6}FA_{0.4}PbI_3$ perovskite devices having different amounts of Al dopants in ZnO as ETL

Al dopant (wt%) in ZnO	Open Circuit Voltage, V_{OC} (mV)	Short Circuit Current Density, J_{SC} (mA/cm^2)	Fill Factor, FF (%)	Efficiency (%)	Series Resistance, R_S (Ω)	Shunt Resistance R_{Sh} (Ω)
0	973.48	21.44	56.69	11.82	10.13	26190
5	992.42	20.16	64.16	12.84	8.96	35800
10	999.38	20.34	66.28	13.48	8.42	25200
15	1004.46	20.18	68.89	13.95	7.05	35700
20	1011.86	19.77	65.52	13.11	10.53	39900

Table S3: Average photovoltaic performance of different compositional mixed organic cation based $MA_xFA_{1-x}PbI_3$ perovskite devices having ZnO and Al doped ZnO (AZO) as ETL

ETL	Mixed Organic Cation Perovskite, $MA_xFA_{1-x}PbI_3$	Open Circuit Voltage, V_{OC} (mV)	Short Circuit Current Density, J_{SC} (mA/cm^2)	Fill Factor, FF (%)	Efficiency (%)	Series Resistance, R_S (Ω)	Shunt Resistance R_{Sh} (Ω)
ZnO	$MAPbI_3$ (x=1)	992.20	19.67	51.32	10.02	8.78	4140
	$MA_{0.8}FA_{0.2}PbI_3$ (x=0.8)	980.55	21.41	53.63	11.26	18.32	36600
	$MA_{0.6}FA_{0.4}PbI_3$ (x=0.6)	973.48	21.44	56.69	11.82	10.13	26190
	$MA_{0.4}FA_{0.6}PbI_3$ (x=0.4)	972.11	21.81	52.15	11.06	12.29	22800
	$MA_{0.2}FA_{0.8}PbI_3$ (x=0.2)	962.52	21.50	50.14	10.34	18.59	29000
	$FAPbI_3$ (x=0)	959.18	21.47	44.98	9.30	18.77	18200
AZO	$MAPbI_3$ (x=1)	1020.18	19.37	65.93	13.03	10.04	41300
	$MA_{0.8}FA_{0.2}PbI_3$ (x=0.8)	1009.63	19.84	67.19	13.46	9.09	42800
	$MA_{0.6}FA_{0.4}PbI_3$ (x=0.6)	1004.46	20.18	68.89	13.95	7.05	35700
	$MA_{0.4}FA_{0.6}PbI_3$ (x=0.4)	994.61	20.29	64.54	13.02	8.87	35000
	$MA_{0.2}FA_{0.8}PbI_3$ (x=0.2)	992.96	20.44	58.07	11.78	12.78	29000
	$FAPbI_3$ (x=0)	982.38	20.50	49.93	10.05	20.84	36700

Table S4: PCE, J_{SC}, V_{OC} and FF values of a batch of 10 (ten) $MA_{0.6}FA_{0.4}PbI_3$/ZnO perovskite devices demonstrating the excellent reproducibility of the fabricated solar cells

Serial No.	Open Circuit Voltage, V_{OC} (mV)	Short Circuit Current Density, J_{SC} (mA/cm^2)	Fill Factor, FF (%)	Efficiency (%)	Series Resistance, R_S (Ω)	Shunt Resistance R_{Sh} (Ω)
1	953.818	20.261	65.99	12.62	5.94	16300
2	978.376	21.952	54.90	11.79	10.62	21200
3	988.187	21.899	55.16	11.94	11.02	35400
4	972.261	21.769	55.02	11.65	11.16	32300
5	992.658	21.324	52.49	11.11	12.20	25000
6	953.609	21.427	58.39	11.81	9.14	20700
7	955.887	21.547	59.35	12.10	8.82	19900
8	988.187	21.899	55.16	11.94	11.03	35400
9	978.341	21.871	55.85	11.95	10.17	23400
10	973.509	20.532	54.66	11.33	11.25	32300

Table S5: PCE, J_{SC}, V_{OC} and FF values of a batch of 10 (ten) $MA_{0.6}FA_{0.4}PbI_3$/AZO perovskite devices demonstrating the excellent reproducibility of the fabricated solar cells

Serial No.	Open Circuit Voltage, V_{OC} (mV)	Short Circuit Current Density, J_{SC} (mA/cm^2)	Fill Factor, FF (%)	Efficiency (%)	Series Resistance, R_S (Ω)	Shunt Resistance R_{Sh} (Ω)
1	995.966	20.822	66.65	13.61	7.83	26800
2	995.31	20.492	68.77	14.03	6.93	30500
3	995.363	20.435	67.70	13.77	8.51	37200
4	989.371	20.263	67.91	13.71	6.39	24400
5	1012.987	19.708	71.34	14.24	5.94	37300
6	1012.505	20.062	67.72	13.76	7.65	41200
7	1013.157	20.005	70.91	14.37	5.94	35000
8	1005.857	19.775	70.99	14.12	5.985	37800
9	1015	20.413	67.83	14.05	8.19	42400
10	1009.113	19.854	69.16	13.86	7.20	44400

Table S6: Fitted values of recombination resistance as a function of applied bias from Nyquist plot in case of $MA_{0.6}FA_{0.4}PbI_3$/ZnO and $MA_{0.6}FA_{0.4}PbI_3$/AZO perovskite devices under dark

Bias (V)	$MA_{0.6}FA_{0.4}PbI_3$/ZnO Device	$MA_{0.6}FA_{0.4}PbI_3$/AZO Device
0.4	74638	88500
0.5	46420	57800
0.6	20100	28500
0.7	6220	9750
0.8	3470	6970
0.9	1820	3872

Table S7: Fitted values of recombination resistance as a function of applied bias from Nyquist plot in case of $MA_{0.6}FA_{0.4}PbI_3$/ZnO and $MA_{0.6}FA_{0.4}PbI_3$/AZO perovskite devices under illumination

Bias (V)	$MA_{0.6}FA_{0.4}PbI_3$/ZnO Device	$MA_{0.6}FA_{0.4}PbI_3$/AZO Device
0.4	7720	12300
0.5	4992	8750
0.6	3030	6100
0.7	2264	4970
0.8	1466	3360
0.9	1110	2770

Table S8: Dark carrier mobility for $MA_{0.6}FA_{0.4}PbI_3$/ZnO devices extracted from Nyquist plot under dark

Bias Voltage (V)	Admittance, Y (μMho) from CPE	Heterogeneity factor, N from CPE	Contact Resistance, R_C (Ω)	Mobility, μ ($cm^2 V^{-1} s^{-1}$)
0.4	0.09	0.95	118	2.13
0.5	0.15	0.94	105	1.62
0.6	0.16	0.97	95	1.21
0.7	0.25	0.96	80	1.07
0.8	0.26	0.98	78	0.82
0.9	0.37	0.96	75	0.79

Table S9: Dark carrier mobility for $MA_{0.6}FA_{0.4}PbI_3$/AZO devices extracted from Nyquist plot under dark

Bias Voltage (V)	Admittance, Y (μMho) from CPE	Heterogeneity factor, N from CPE	Contact Resistance, R_C (Ω)	Mobility, μ ($cm^2 V^{-1} s^{-1}$)
0.4	0.07	0.96	114	2.61
0.5	0.10	0.96	107	1.89
0.6	0.14	0.95	97	1.72
0.7	0.21	0.95	93	1.24
0.8	0.25	0.96	87	0.98
0.9	0.33	0.96	80	0.82

Dark Carrier Mobility Calculation:

Dark carrier mobility was calculated from the fitted electronic parameters from Nyquist plot. The dark carrier mobility can be expressed as:

Mobility, $\mu = \frac{\tau_t q l^2}{kT}$ [1]

where, τ_t, q, l, k and T denote transit time, elementary charge, perovskite layer thickness, Boltzman's constant and absolute temperature respectively.

Transit time, τ_t can be defined as:

Transit time, $\tau_t = R_C C_\mu$ [1]

Where, R_C and C_μ denote contact resistance and chemical capacitance respectively. C_μ can be found by the conversion of constant phase element (CPE) into capacitance using the following formula:

$C_\mu = \left(R_{Rec}\right)^{\frac{1-N}{N}} \left(Q\right)^{\frac{1}{N}}$ [2]

$$Q = \frac{Y}{2\pi f}$$

where, C_μ, Q, N, Y and f denote converted capacitance from constant phase element (CPE), pseudo capacitance from CPE, ideality factor from CPE, admittance from CPE and source frequency for impedance analyzer respectively.

Table S10: Flat-band potential, acceptor density and depletion layer width at zero bias of $MA_{0.6}FA_{0.4}PbI_3$/ZnO and $MA_{0.6}FA_{0.4}PbI_3$/AZO perovskite devices extracted from Mott-Schottky curve

ETL Layer	Dopant Density (cm^{-3})	Flat-band Potential (V)	Depletion Layer Width (nm)
Pristine ZnO	2.0×10^{16}	0.96	335.46
Al doped ZnO (AZO)	6.2×10^{16}	1.13	206.80

Table S11: PCE, J_{SC}, V_{OC} and FF values of $MA_{0.6}FA_{0.4}PbI_3$/ZnO and $MA_{0.6}FA_{0.4}PbI_3$/AZO perovskite devices at two different scan rates demonstrating the hysteresis phenomena in the corresponding devices

ETL Layer	Scan rate (V/s)	Open Circuit Voltage, V_{OC} (mV)	Short Circuit Current Density, J_{SC} (mA/cm^2)	Fill Factor, FF (%)	Efficiency (%)	Series Resistance, R_S (Ω)	Shunt Resistance R_{Sh} (Ω)
Pristine ZnO	0.1	977.884	22.157	58.08	12.35	9.59	30200
	1.0	978.341	21.871	55.85	12.00	10.20	23400
Al doped ZnO (AZO)	0.1	1013.157	20.005	70.91	14.37	5.94	35000
	1.0	1012.755	20.158	69.81	14.25	6.80	35900

Table S12: Day wise PCE, J_{SC}, V_{OC} and FF values of $MA_{0.6}FA_{0.4}PbI_3$/ZnO devices stored in a N_2 filled glovebox for 30 days

No. of Days	Open Circuit Voltage, V_{OC} (mV)	Short Circuit Current Density, J_{SC} (mA/cm^2)	Fill Factor, FF (%)	Efficiency (%)	Series Resistance, R_S (Ω)	Shunt Resistance R_{Sh} (Ω)
0	978.376	21.952	54.90	11.79	10.6	21200
2	977.884	22.157	58.08	12.58	9.585	30200
3	984.247	22.396	60.66	13.37	9.09	23200
4	984.398	21.703	59.65	12.74	9.315	28500
6	986.650	21.437	62.35	13.19	7.695	25700
8	982.346	21.218	60.57	12.62	9.045	33100
10	967.403	21.153	53.93	11.04	12.06	19900
12	977.186	20.798	56.50	11.48	10.665	28400
13	984.446	20.833	55.35	11.35	11.34	22300
14	990.760	20.414	56.18	11.36	10.8	13700
16	991.085	19.914	51.58	10.18	14.31	18500
19	991.420	18.043	53.27	9.53	13.365	9620
21	994.785	16.699	50.74	8.43	16.74	9360
24	972.980	14.588	48.48	6.88	20.34	8780
25	989.400	10.951	51.88	5.62	20.21	9610
27	983.275	10.377	45.36	4.63	35.96	9680
30	982.352	9.509	44.88	4.19	40.95	11900

Table S13: Day wise PCE, J_{SC}, V_{OC} and FF values of $MA_{0.6}FA_{0.4}PbI_3$/AZO devices stored in a N_2 filled glovebox for 30 days

No. of Days	Open Circuit Voltage, V_{OC} (mV)	Short Circuit Current Density, J_{SC} (mA/cm^2)	Fill Factor, FF (%)	Efficiency (%)	Series Resistance, R_S (Ω)	Shunt Resistance R_{Sh} (Ω)
0	991.513	20.393	66.96	13.54	8.01	27700
1	1016.040	19.374	69.80	13.74	6.30	37900
2	1009.113	19.854	69.16	13.86	7.20	44400
4	1013.220	19.659	71.56	14.25	5.76	35800
5	997.213	19.852	71.09	14.07	5.58	35700
7	991.436	19.964	71.05	14.06	4.91	32700
9	997.103	19.430	71.95	13.94	4.55	51600
11	996.940	19.623	70.52	13.80	4.68	27100
13	996.090	19.754	68.89	13.56	5.18	29200
16	993.480	18.957	65.87	12.41	6.35	42100
18	981.971	19.235	62.98	11.90	6.39	26700
20	985.576	18.870	61.96	11.52	7.02	31000
22	971.362	18.755	58.64	10.68	8.64	23700
24	960.592	18.400	57.48	10.16	8.10	16800
27	952.135	17.789	56.55	9.58	8.55	13900
29	954.644	17.056	56.56	9.21	9.23	13200
30	924.941	17.527	55.20	8.95	10.13	20100

Table S14: Fitted values of different parameters from Nyquist plot of the degraded (30 days) $MA_{0.6}FA_{0.4}PbI_3$/ZnO and $MA_{0.6}FA_{0.4}PbI_3$/AZO devices at 0.85V under dark

ETL Layer	R_C (Ω)	R_{Rec} (Ω)	C_C (nF)	CPE-Y(nMho)	CPE-N
Pristine ZnO	127	3050	15.3	0.28	0.95
Al doped ZnO (AZO)	98	5940	13.5	1.54	0.96

Table S15: Flat-band potential, acceptor density and depletion layer width at zero bias of degraded (30 days) $MA_{0.6}FA_{0.4}PbI_3$/ZnO and $MA_{0.6}FA_{0.4}PbI_3$/AZO devices extracted from Mott-Schottky curve

ETL Layer	Dopant Density (cm^{-3})	Flat-band Potential (V)	Depletion Layer Width (nm)
Pristine ZnO	$4.17x10^{16}$	0.63	188.29
Al doped ZnO (AZO)	$6.63x10^{16}$	0.96	172.37

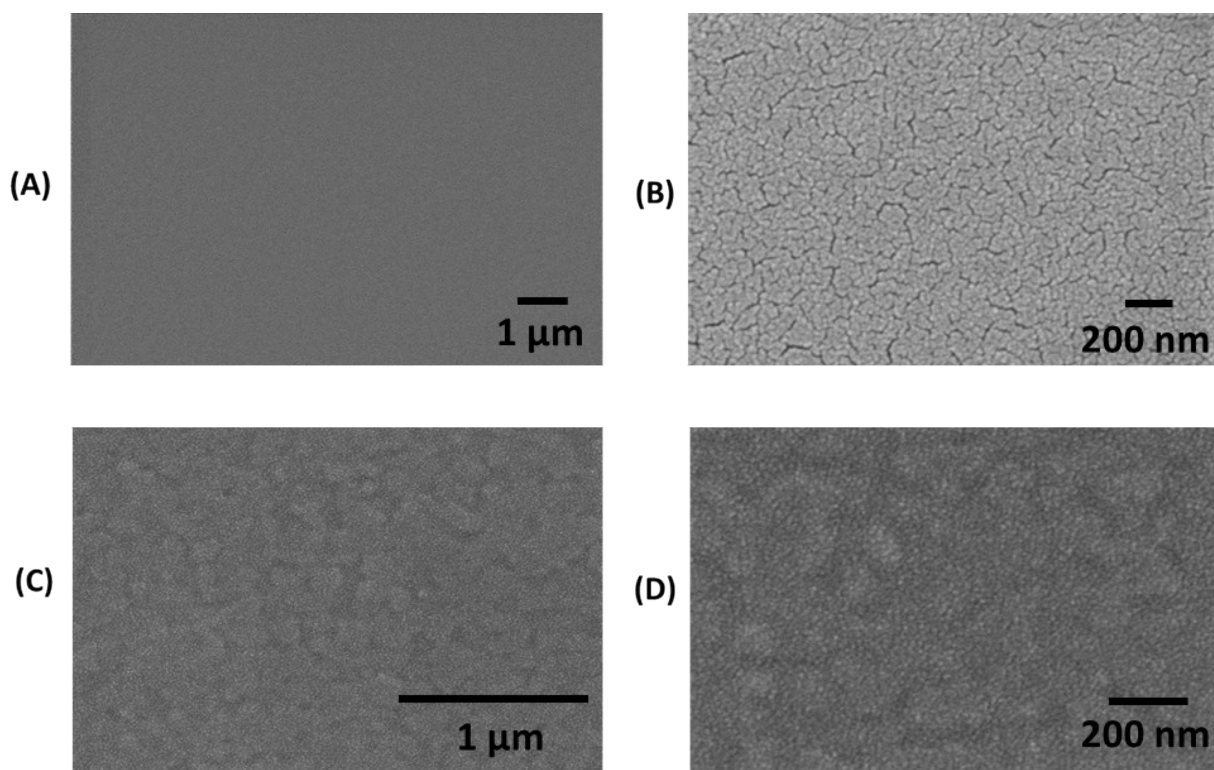

Fig. S1 Top view Scanning Electron Microscopy (SEM) images of (A)-(B) ZnO film and (C)-(D) AZO film on top of ITO/glass substrate

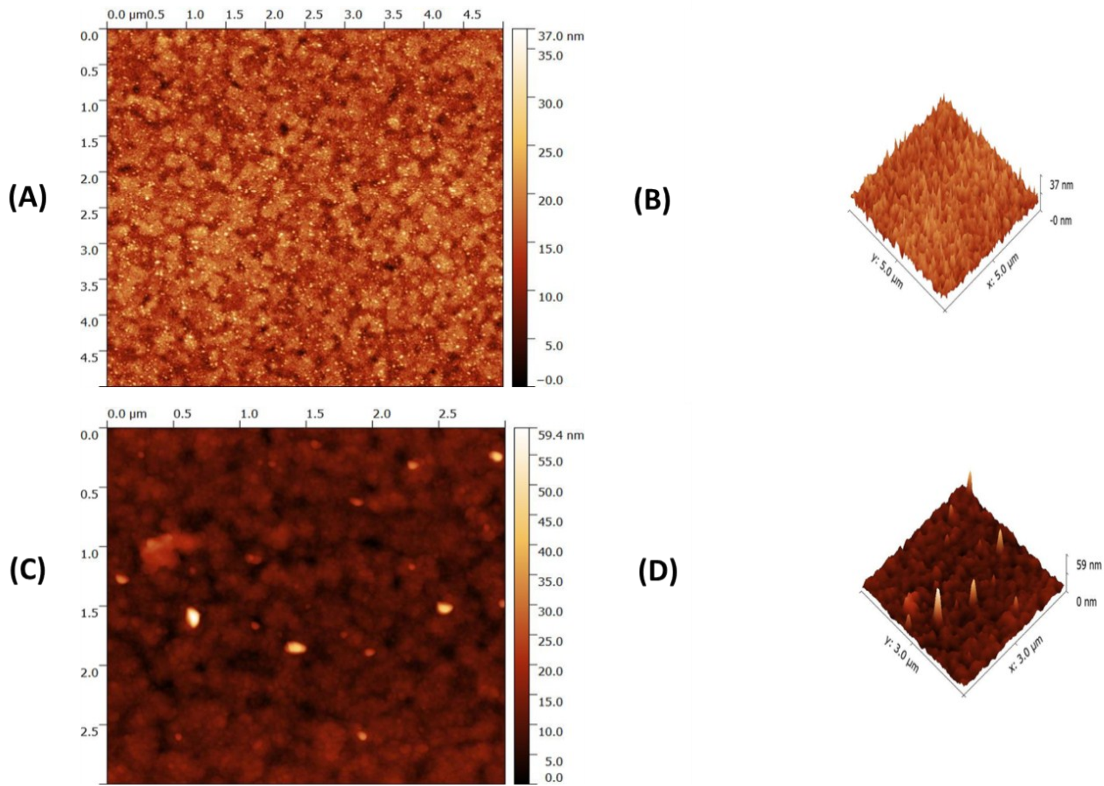

Fig. S2 Two and Three dimensional Atomic Force Microscopy (AFM) images (A)-(B) ZnO film and (C)-(D) AZO film on top of ITO/glass substrate

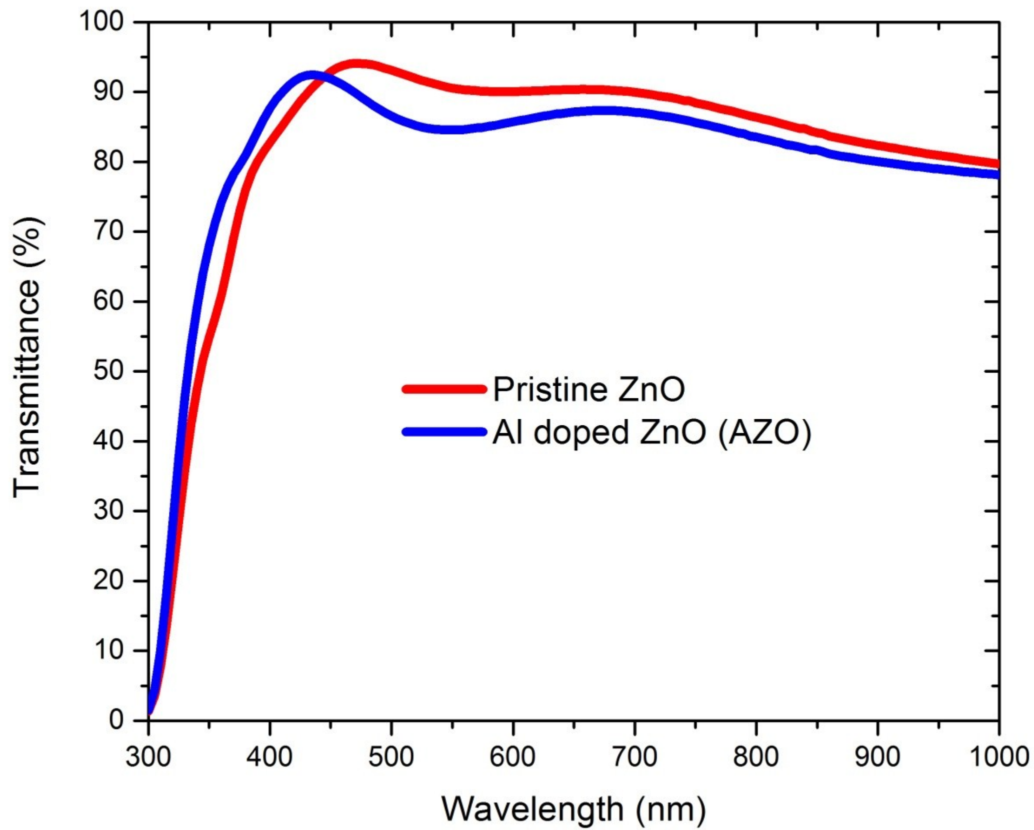

Fig. S3 Transmittance pattern of low temperature processed pristine ZnO and AZO ETL films on ITO/glass substrate

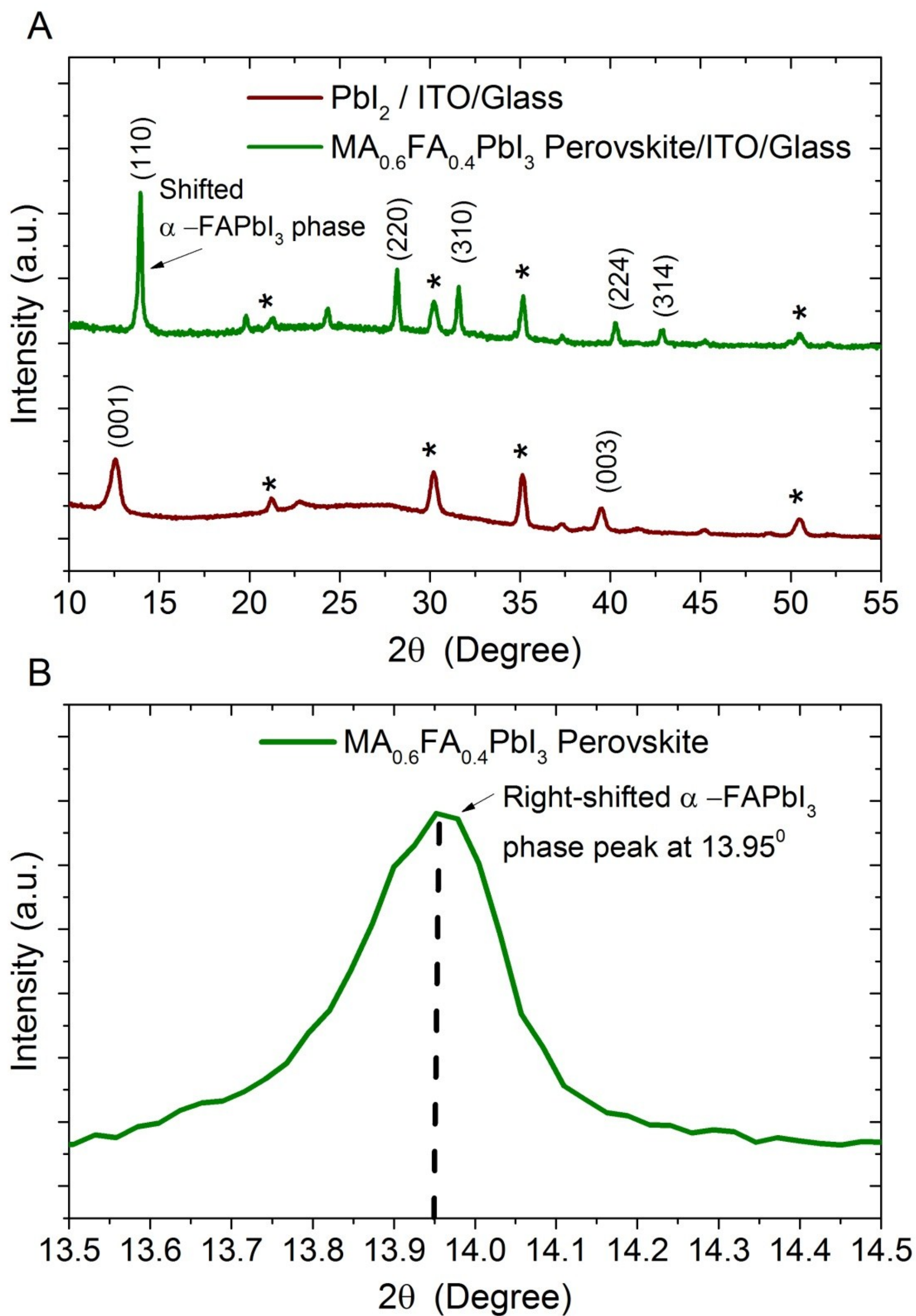

Fig. S4 (A) XRD patterns of PbI_2 and $MA_{0.6}FA_{0.4}PbI_3$ perovskite showing the major diffraction peaks and the corresponding crystal orientation (B) Enlarged view of the XRD pattern of $MA_{0.6}FA_{0.4}PbI_3$ lifting up the 0.15^0 right-shift in $MA_{0.6}FA_{0.4}PbI_3$ perovskite peak with regards to pristine $FAPbI_3$ α-phase peak at 13.80^0 (*The * signs denote the peaks for ITO*)

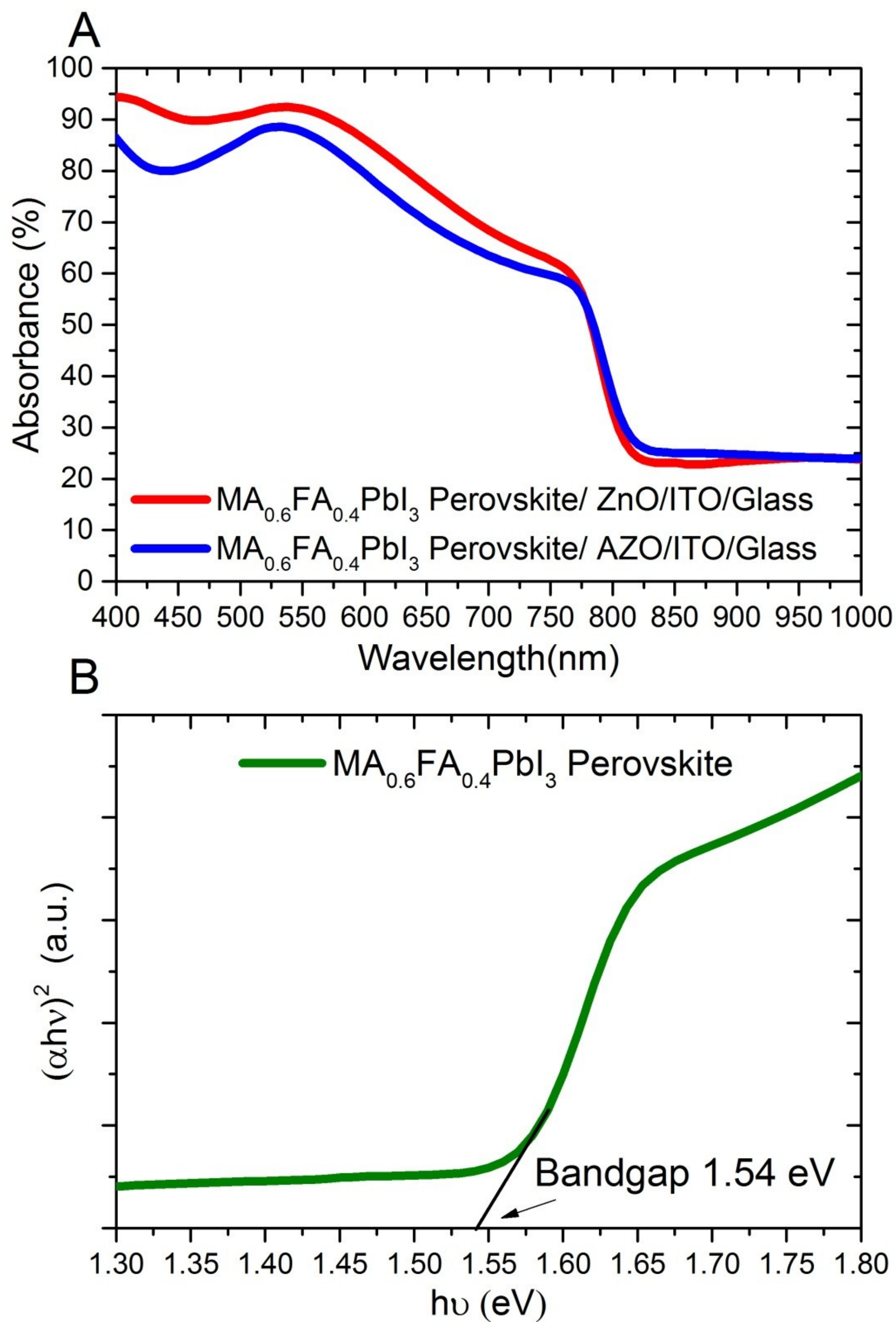

Fig. S5 (A) Absorption curves of $MA_{0.6}FA_{0.4}PbI_3$/ZnO and $MA_{0.6}FA_{0.4}PbI_3$/AZO films on top of ITO/glass substrate (B) Estimation of approximate material bandgap of $MA_{0.6}FA_{0.4}PbI_3$ perovskite film using Tauc plot

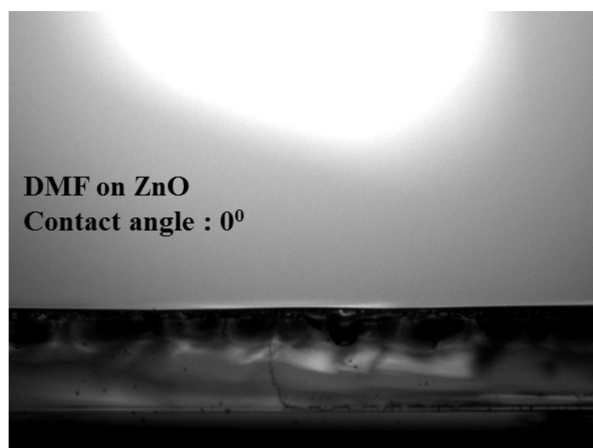

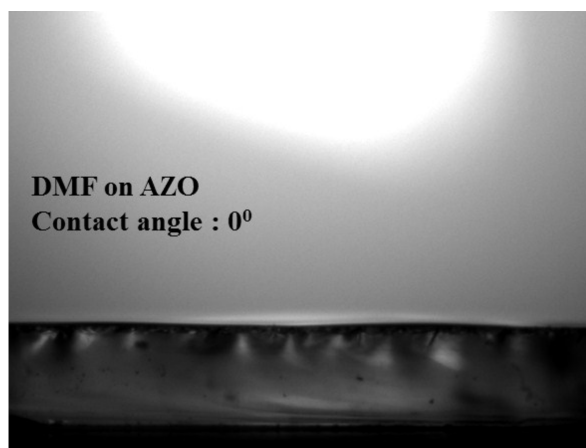

(A) **(B)**

Fig. S6 Contact angle measurement with DMF solution (PbI_2 precursor) on (A) pristine ZnO and (B) Al doped ZnO (AZO) film. Both the contact angles were essentially ~0^0 indicating that the surface wettability of ETL films (ZnO or AZO film) does not substantially contribute to the variation in surface morphology of overlying perovskite layer

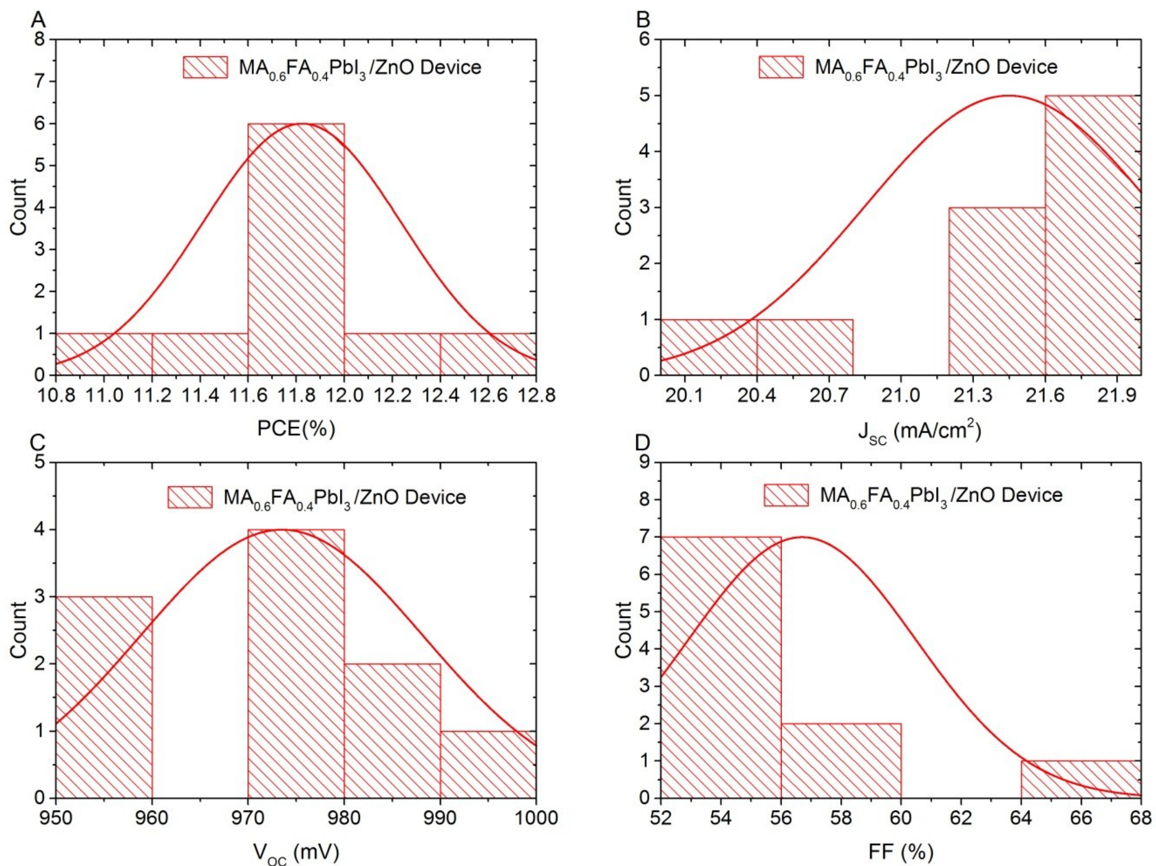

Fig. S7 Statistical histogram (showing normal distribution) of (A) PCE, (B) J_{SC}, (C) V_{OC} and (D) FF obtained from 10 identically fabricated ITO/solgel ZnO/ $MA_{0.6}FA_{0.4}PbI_3$ perovskite/Spiro-OMeTAD/Ag devices in a single batch

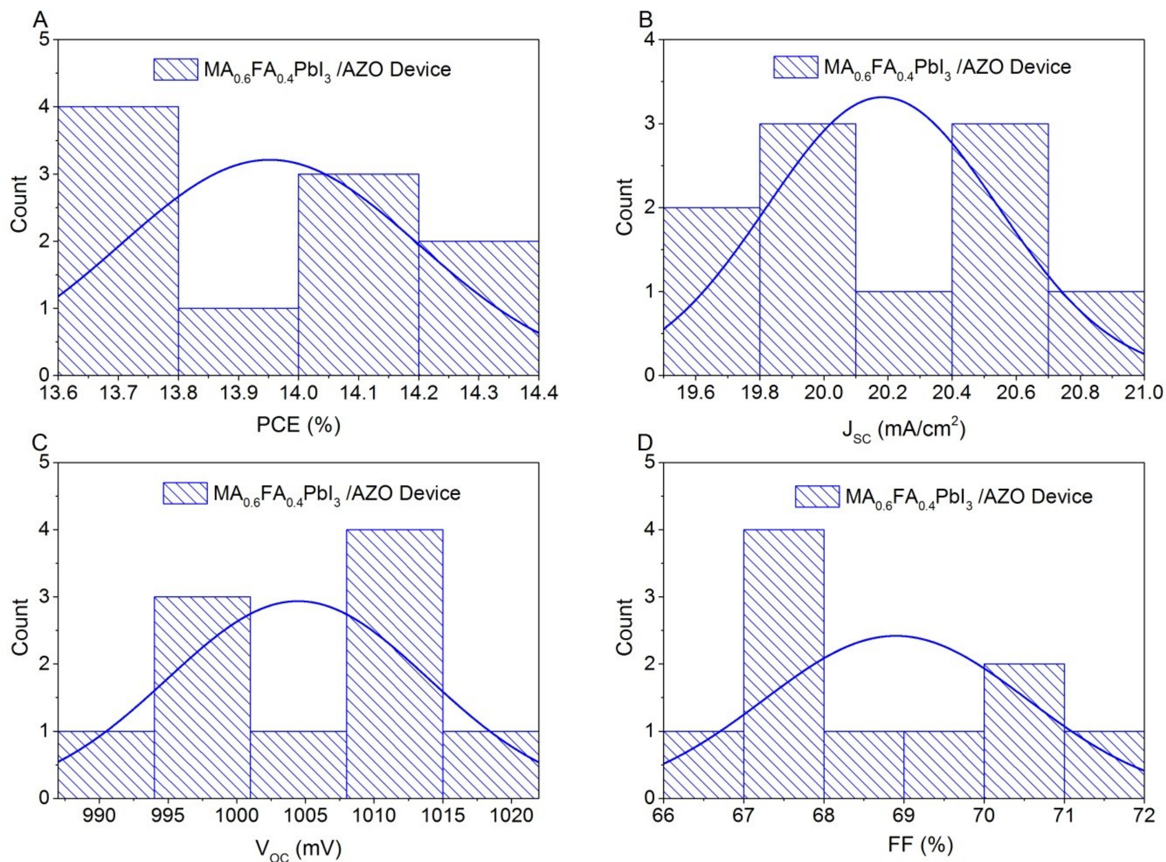

Fig. S8 Statistical histogram (showing normal distribution) of (A) PCE, (B) J_{SC}, (C) V_{OC} and (D) FF obtained from 10 identically fabricated ITO/AZO/ $MA_{0.6}FA_{0.4}PbI_3$ perovskite/Spiro-OMeTAD/Ag device in a single batch

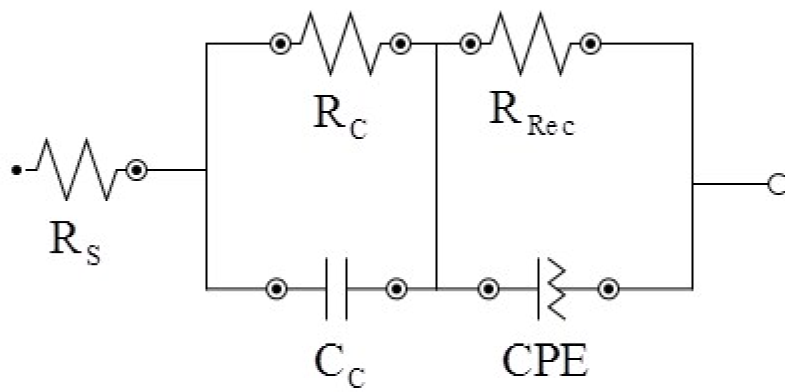

Fig. S9 Equivalent circuit model used to fit the experimental data from Nyquist plot

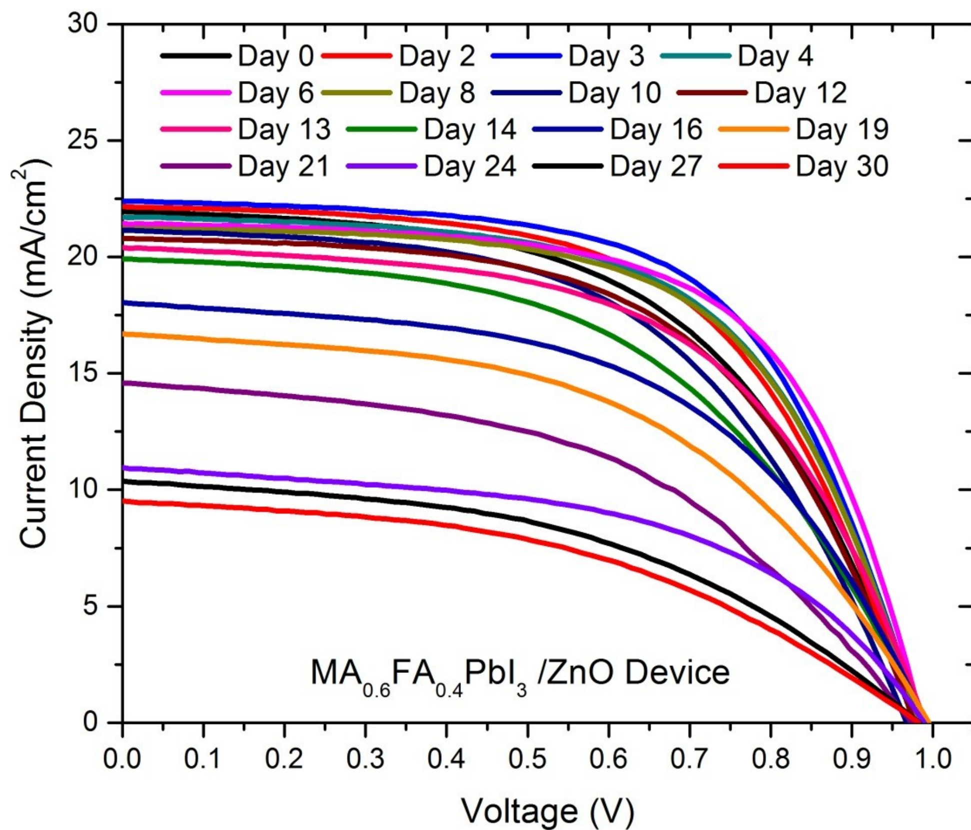

Fig. S10 IV curves of $MA_{0.6}FA_{0.4}PbI_3$/ZnO devices throughout the time period of degradation study (30 days) with certain intervals

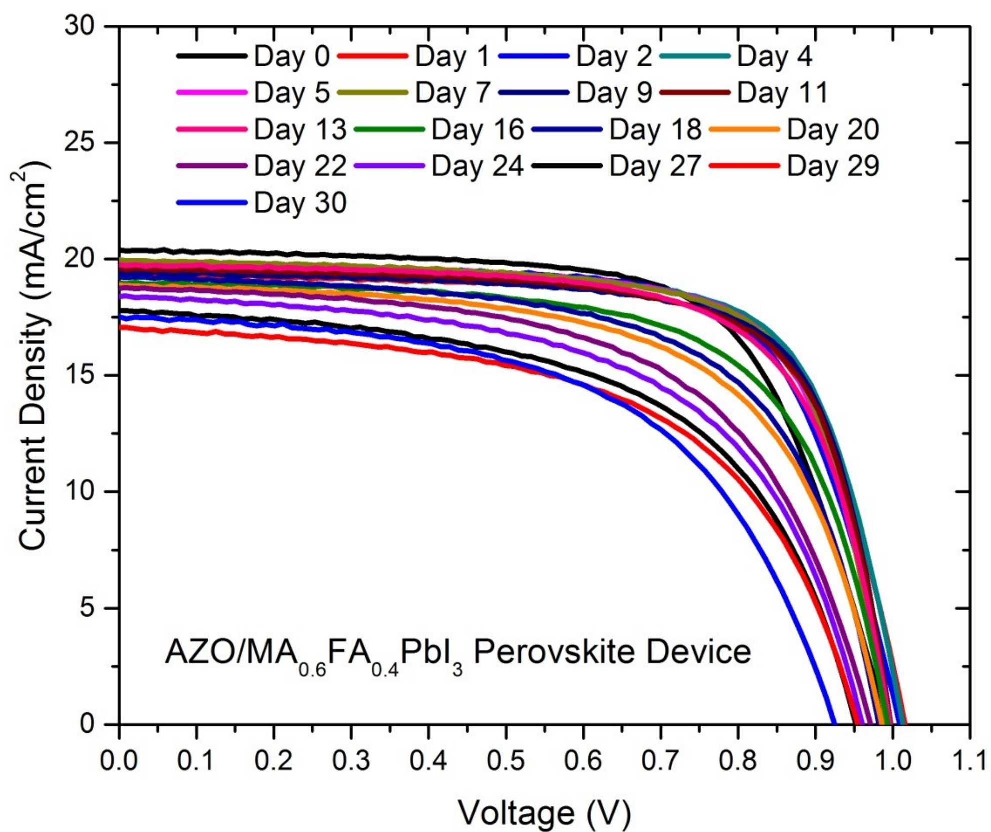

Fig. S11 IV curves of $MA_{0.6}FA_{0.4}PbI_3$/AZO devices throughout the time period of degradation study (30 days) with certain intervals

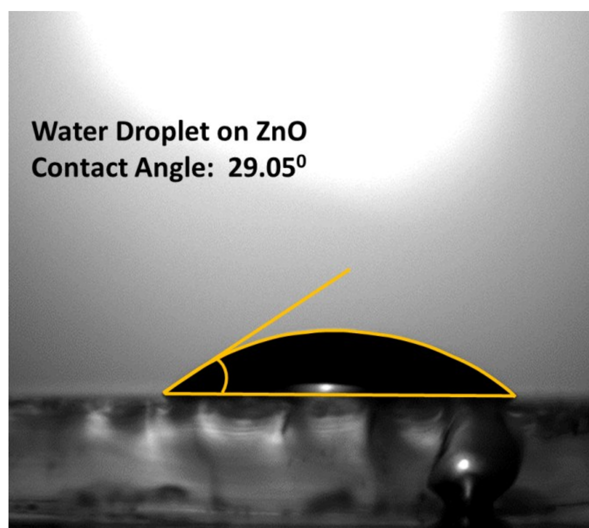

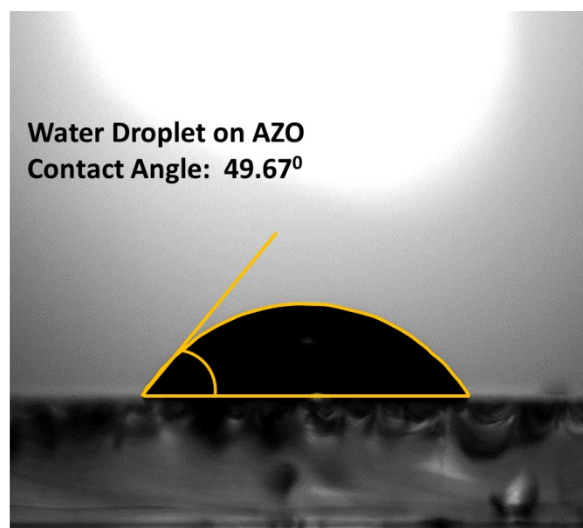

(A)

(B)

Fig. S12 Contact angle measurement with water droplet on (A) pristine ZnO and (B) Al doped ZnO (AZO) film. The contact angle of water on pristine ZnO and AZO film are 29.05^0 and 49.67^0 respectively, indicating AZO film is less hydrophilic or more hydrophobic

References:

[1] G. Garcia-Belmonte, A. Munar, E.M. Barea, J. Bisquert, I. Ugarte, R. Pacios, Organic Electronics, 9 (2008) 847-851.
[2] C.M. Gore, J.O. White, E.D. Wachsman, V. Thangadurai, Journal of Materials Chemistry A, 2 (2014) 2363-2373.